FERROELECTRICS
2020, VOL. 569, 201–208
https://doi.org/10.1080/00150193.2020.1822677

Taylor & Francis
Taylor & Francis Group

Dielectric and local piezoelectric properties of lead-free KNN-based perovskite ceramics

E. D. Politova[a], G. M. Kaleva[a], A. V. Mosunov[b], N. V. Sadovskaya[c], D. A. Kiselev[d], A. M. Kislyuk[d], T. S. Ilina[d], and S. Yu. Stefanovich[b]

[a]Semenov Institute of Chemical Physics, Russian Academy of Sciences, Moscow, Russia; [b]Lomonosov Moscow State University, Moscow, Russia; [c]Federal Scientific Research Center «Crystallography and Photonics», Russian Academy of Sciences, Moscow, Russia; [d]National University of Science and Technology "MISiS", Moscow, Russia

ABSTRACT
Influence of cation substitutions in $(K_{0.5}Na_{0.5})NbO_3$–$Ba(Li_{2/5}W_{3/5})O_3$ ceramics on structure parameters, microstructure, dielectric, ferroelectric and local piezoelectric properties have been studied. Depending on solid solutions compositions, changes in structure parameters and effective d_{33} piezoelectric coefficient and other properties were observed.

ARTICLE HISTORY
Received 24 September 2019
Accepted 25 May 2020

KEYWORDS
Perovskite structure; sodium-potassium niobate; dielectric; ferroelectric; local piezoelectric properties

Introduction

Perovskite oxides based on potassium-sodium niobate $(K,Na)NbO_3$ (KNN) are among the most intensively studied last ten years as promising materials for replacement of PZT materials containing toxic lead oxide [1–16].

Main endeavors for the development of new piezoelectric materials are mostly focused on modifications of compositions close to the morphotropic phase boundary (MPB). This approach was effectively used for PZT materials. In the case of KNN, compositions along with cation substitutions lead to a shift of the MPB position and a shift of the transition temperature from the orthorhombic to tetragonal phase at room temperature [5–9,11]. Special problems were determined by difficulties in the preparation of KNN-based stoichiometric compositions due to the narrow sintering temperature interval [9–16].

In this work, the effects of the modification of compositions by cation substitutions in A- and B-sites of KNN perovskite lattice on structure, microstructure, dielectric, ferroelectric and local piezoelectric properties of $(1\text{-}x)(K_{0.5}Na_{0.5})NbO_3$–$xBa(Li_{2/5}W_{3/5})O_3$ ceramics have been studied.

Experimental

Ceramic samples $(1\text{-}x)(K_{0.5}Na_{0.5})NbO_3$–$xBa(Li_{2/5}W_{3/5})O_3$ (KNN-BLW) with ($x = 0$–0.1, $\Delta x = 0.02$) were prepared by the solid-state reaction method with calcination

CONTACT E. D. Politova politova@nifhi.ru
This paper was presented at the International Scientific and Practical Conference "Multiferroics: Fabrication, Properties, Applications" held in Vitebsk, Russia on September 24–27, 2019.

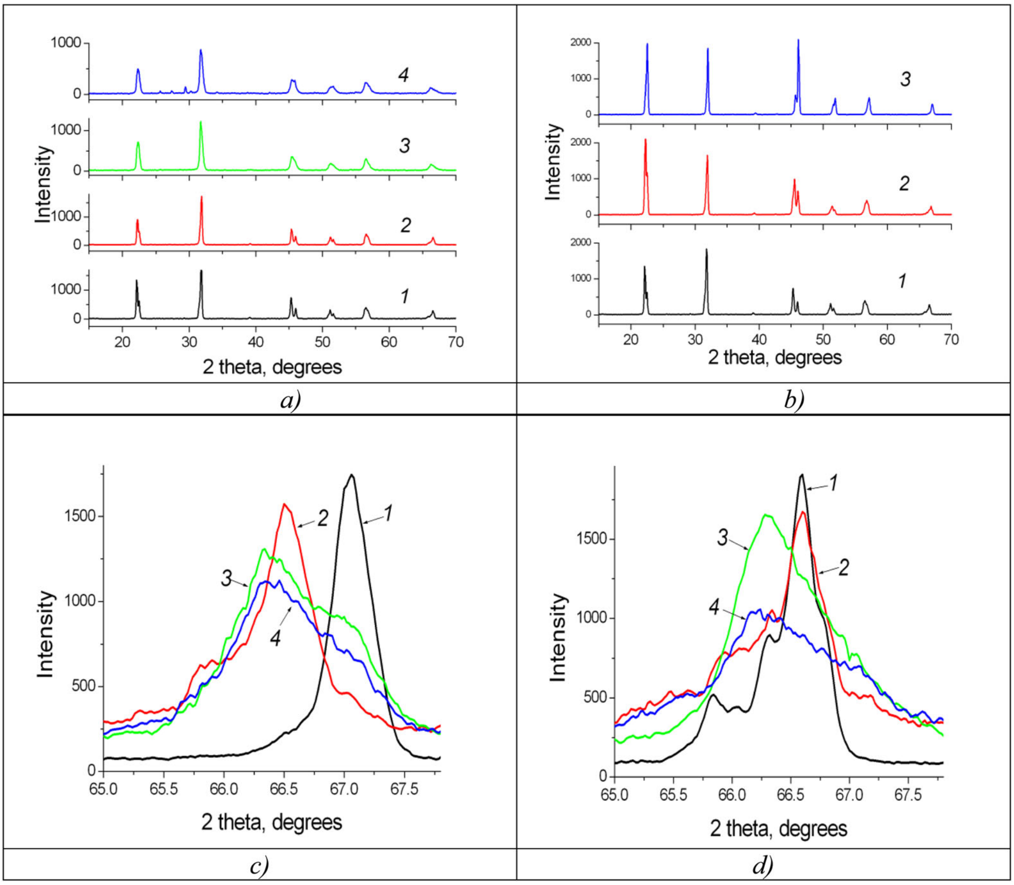

Figure 1. a) X-ray diffraction patterns of the KNN-BLW samples with $x = 0.0$ (1), 0.02 (2), 0.04 (3), 0.06 (4) sintered at 1448 K (2 h); b) of the KNN samples sintered at 1373 K (1), 1423 K (2), 1448 K (3); c, d) parts of the X-ray diffraction patterns of the samples with $x = 0.0$ (1), 0.02 (2), 0.04 (3), 0.06 (4) sintered at 1448 K (2 h) and 1373 K (2 h), respectively.

temperatures of $T_1 = 1073$ K (6 h), and sintering temperatures of $T_2 = 1273–1448$ K (2 h) using as initial reagents carbonates K_2CO_3, Na_2CO_3, Li_2CO_3 and $BaCO_3$, oxides Nb_2O_5 and WO_3 (all "pure grade"). After synthesis, some samples were additionally modified by 5 w. % of LiF additives with low melting temperature (1143 K) in order to improve sintering of ceramics [15,16].

Phase content and structure parameters of the samples were characterized by the x-ray diffraction method (DRON-3M, Cu-K_α radiation with wavelength $\lambda = 1.5405$ A, 2 theta range of 5–80 degrees).

The microstructure of the samples was examined by the scanning electron microscopy (SEM) method using the JEOL YSM-7401F with a JEOL JED-2300 energy dispersive x-ray spectrometer system.

The second harmonic generation (SHG) method was used to characterize spontaneous polarization and phase transitions in the samples using Nd:YAG laser, $\lambda = 1.064\,\mu$m in the reflection.

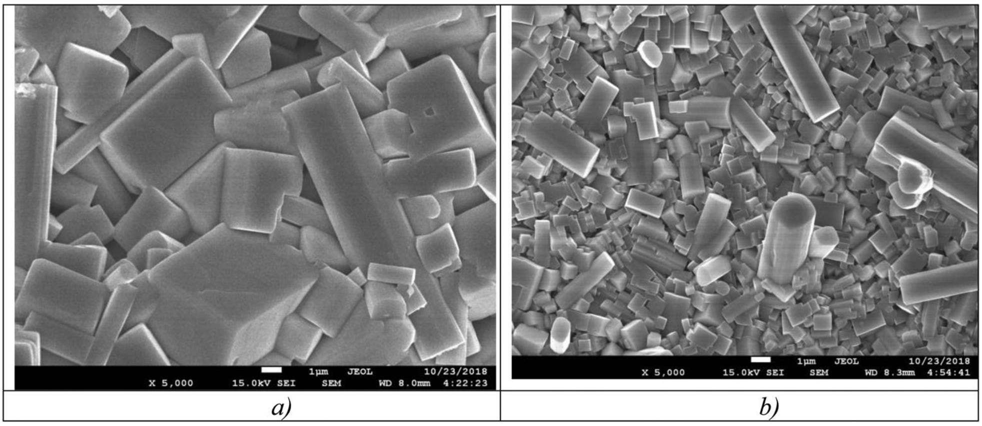

Figure 2. Microstructure of the samples doped by LiF sintered at 1373 K (2 h) with $x = 0.02$ (a) and 0.06 (b). Bars = 1 μm.

Piezoresponse force microscopy (PFM) studies were carried out using an MFP-3D (Asylum Research, Oxford Instruments, Santa Barbara, CA) with a TiIr coated Si cantilever (Asyelec-02) and a nominal 42 N/m spring constant. An AC voltage (1-2 V_{pp}) was superimposed onto a triangular square-stepping wave ($f = 0.5$ Hz, with writing and reading times 25 ms, and bias window up to ± 30 V) during the remnant piezoelectric hysteresis loops measurements. To estimate the effective d_{33} piezoelectric constants, the deflections and vibration sensitivity of the cantilever alignment were calibrated by GetReal procedure using IgorPro software (Asylum Research, Oxford Instruments).

Results and discussion

Pure perovskite samples with the orthorhombic structure were prepared using synthesis at $T_1 = 1100$ K and sintering at $T_2 = 1373–1448$ K (Figure 1a). Only small amounts of admixture phase $K_2Nb_8O_{21}$ were observed in the X-ray diffraction patterns of the samples with $x = 0.1$. It should be noted that texturing effects were observed with sintering temperature increasing (Figure 1b). A slight shift of the x-ray diffraction peaks to smaller angles was observed with x increasing (Figure 1c,d). This points to a decrease in the unit cell volume due to introduction of aliovalent cations with smaller average radii into A- and B-positions of perovskite lattice.

The microstructure of the samples is also sensitive to cation substitutions (Figure 2). Mean size of grains decreased with x increasing while slight enlargement of the mean size of grains was observed with sintering temperature increasing.

In the dielectric permittivity versus temperature curves, steps near ~400–450 K and maxima at ~650–680 K were revealed (Figure 3). A slight decrease in temperatures of both phase transitions was observed for the samples studied. A decrease in the ε_{RT} and tanδ values in compositions with $x = 0–0.06$ (Figure 4a) correlates with a decrease in the SHG signal proportional to the spontaneous polarization value measured for ceramics sintered at 1175 K (Figure 4b, curve 3), while a further slight increase in the ε_{RT} and tanδ values may be explained by an increase in total electroconductivity of the samples with $x > 0.06$ (Figure 4a). Moreover, these effects are related to the appearance of

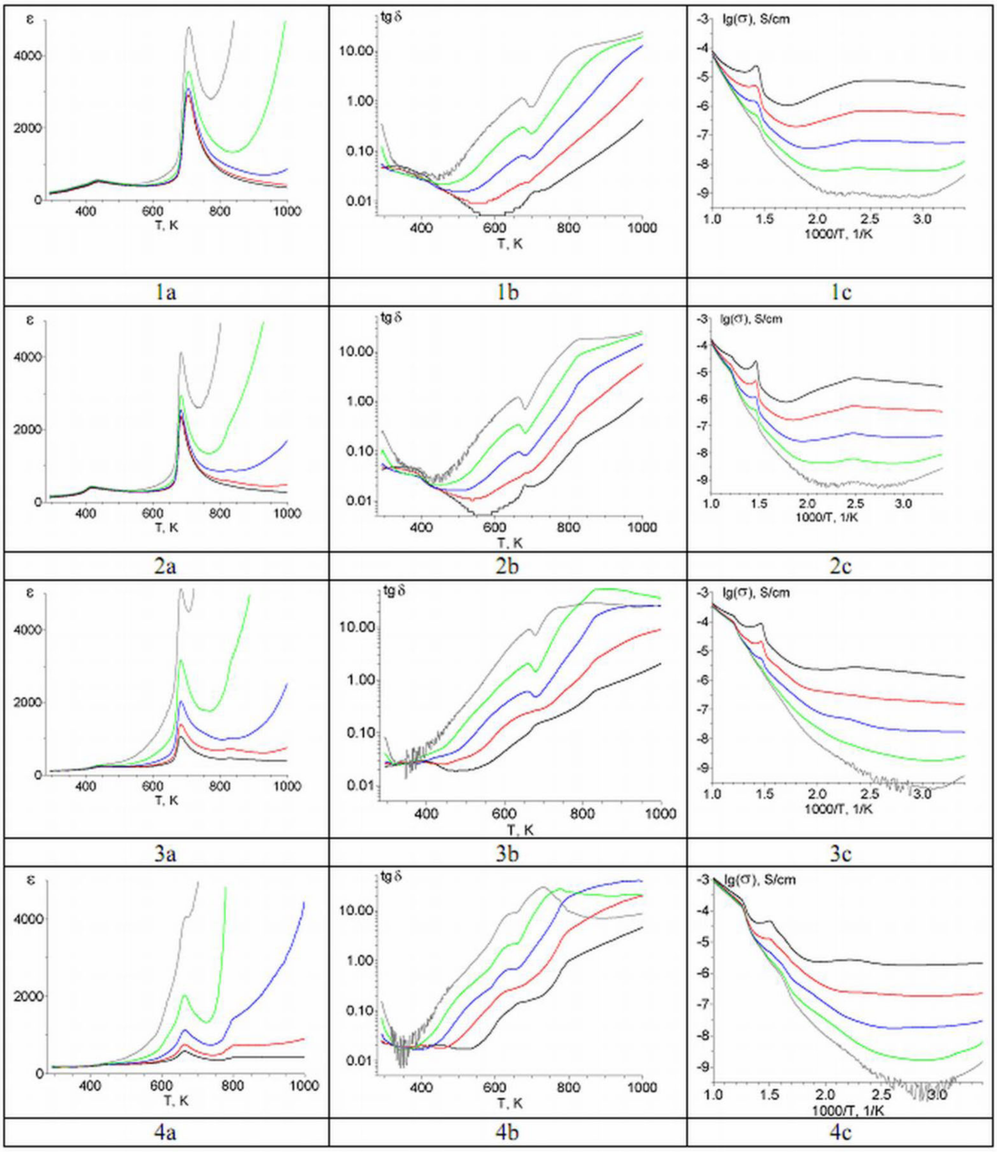

Figure 3. Temperature dependences of dielectric permittivity $\varepsilon(T)$ (a), dielectric loss tan δ(T) (b) and lg $\sigma(1000/T)$ (c) of the samples with $x = 0.0$ (1a-c), 0.02 (2a-c), 0.06 (3a-c), 0.10 (4a-c) doped with 5 w.% LiF sintered at $T_2 = 1373$ K (2 h) measured at frequencies $f = 100$ Hz, 1,10,100 kHz, 1 MHz.

additional anomalies in the $\varepsilon(T)$ curves near 800 K which points to the formation of dipoles relaxing in an alternative field due to oxygen deficiency stimulated by K and/or Na loss at sintering (Figure 3, curves 3a and 4a).

The SHG measurements confirmed the polar nature of the samples reflecting their ferroelectric properties (Figure 4b). With increasing BLW content, decrease in intensity of the SHG signal was observed in samples with $x > 0.04$ sintered at different temperatures.

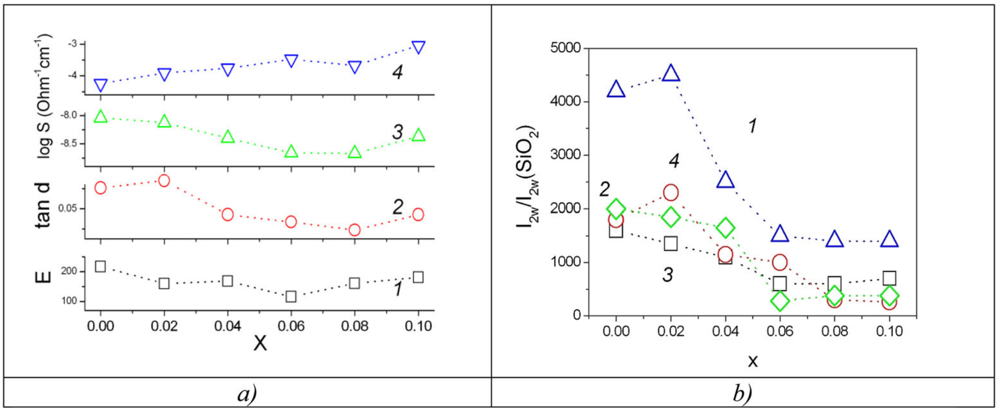

Figure 4. a) Concentration dependences of dielectric permittivity ε_{RT} (1), dielectric loss tan δ (2) and lg σ at the room temperature (3) and at 1000 K (4) of the samples with $x = 0.0$–0.1 doped with 5 w. % LiF sintered at T_2=1373 K (2 h) measured at frequency $f = 1$ kHz; b) Concentration dependence of the SHG signal for the KNN-BLW samples sintered at $T_2 = 1272$ K (8 h) (1), 1373 K (2 h) (2), 1373 K (2 h) doped by with LiF (3), 1448 K (2 h) (4).

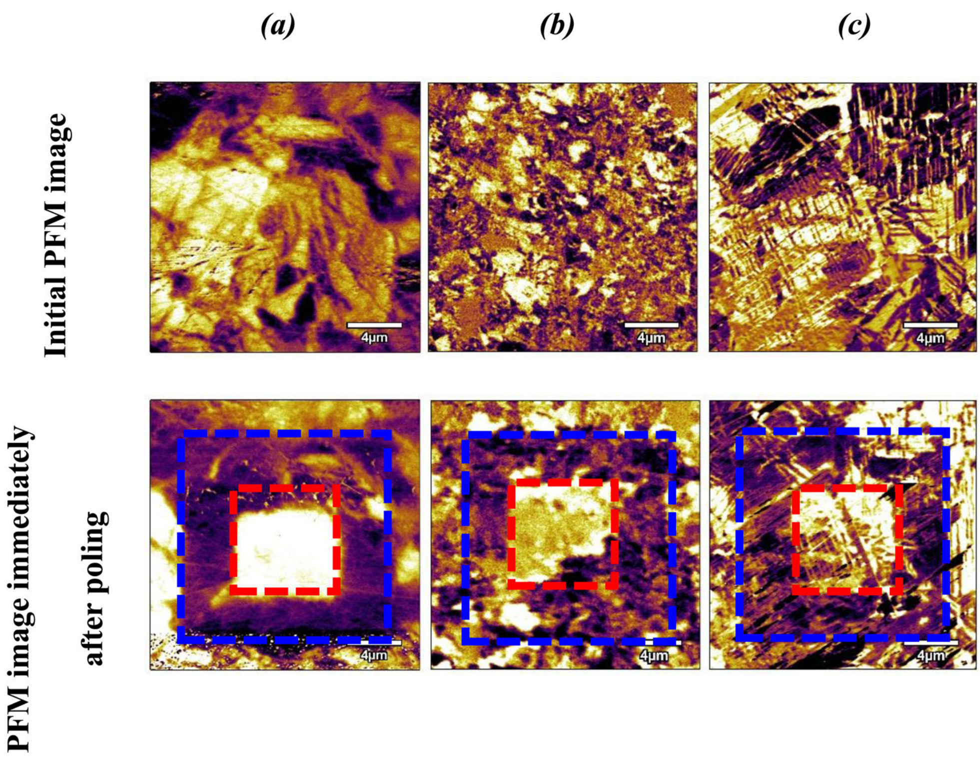

Figure 5. Initial domain structure and PFM images of polarized ceramics with $x = 0.0$ (a), 0.02 (b), and 0.06 (c).

Figure 5 (top row) depicts the initial domain structure of the KNN ceramic with different concentration of BLW with a scan size of 20 μm; the topography is not shown because it does not provide additional information. Complex domain structure

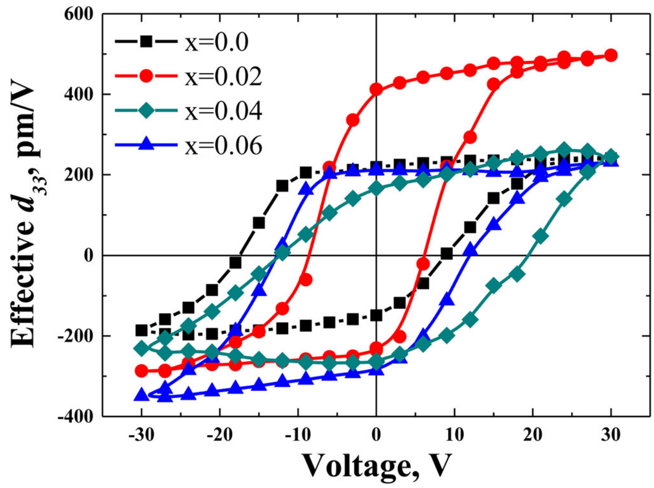

Figure 6. Remnant effective d_{33} (V) piezoelectric hysteresis loops of the KNN-BLW samples with $x = 0.0$, 0.02, 0.04 and 0.06.

consisting of multiple domain patterns, was found for ceramics with $x = 0.0$ and $x = 0.02$. Simultaneously, with x increasing to 0.02, the ferroelectric domain size decreased to 1–2 µm compared with $x = 0.0$ composition. Note that the island domains for composition with $x = 0.06$ are composed of finer stripe domains with the width in the range of 200–300 nm.

To study the effect of the electric field on the domain structure, two square areas of 15×15 µm and 7.5×7.5 µm (structure "box-in-box") were scanned under a DC voltage of -30 V and $+30$ V applying to the cantilever, respectively (Figure 5, bottom row). In the PFM images, areas with dark contrast represented domains with upward polarization orientation, while areas with bright contrast represented the opposite case. For the pure KNN ceramic, the piezoresponse image under ±30 V indicated the polarization switched more completely and the domain structure became more stable. In the samples with $x = 0.02$ and 0.06, only partial ferroelectric domain could be induced. Here it should be noted that incomplete domain switching was a combined effect of the polarization switching and the domain relaxation. Taking into account these effects, the poling behavior could be compared among these three representative compositions which indicated that the KNN samples with higher x required higher electric field to realize the domain switching.

In order to further investigate the domain switching at nanoscale of the KNN-BLW ceramic, remnant PFM hysteresis loops were measured, as shown in Figure 6. It should be noted that in the samples studied the values of effective d_{33} measured at $+30$ V do not coincide with d_{33} values recorded at -30 V. Such effect may be explained by the presence of non-180° domains in ceramics [17]. Furthermore, remnant loops shift toward the negative voltage, indicating that internal bias field exists in ceramics. The highest effective d_{33} piezoelectric coefficient values reached high values $\sim$400 pm/V at $V_{DC} = 30$ V and small coercive voltage in the samples with $x = 0.02$ (Figure 6). These data correlate with concentration dependences of spontaneous polarization (Figure 4b).

Conclusions

Structure, microstructure, dielectric, ferroelectric and piezoelectric properties of the (1-x)($K_{0.5}Na_{0.5}$)NbO_3–xBa($Li_{2/5}W_{3/5}$)O_3 ($x = 0$–0.1) ceramics were studied. Slight changes in the unit cell volume and temperatures of phase transitions were observed depending on composition and sintering conditions. The highest values of the effective d_{33} piezoelectric coefficients ~400 pm/V were observed for ceramics with $x = 0.02$. This confirms prospects of these compositions for the development of new efficient piezoelectric materials.

Funding

The work was supported by the Russian Foundation for Basic Research (Project 18-03-00372) and by the Ministry of Science and Higher Education of the Russian Federation within the framework of the state assignment in the field of science (basic research, project No. 0718-2020-0031) and due to the subsidy allocated by the FIC of the Semenov Institute of Chemical Physics of the Russian Academy of Sciences to carry out state assignment on the topic No. 45.22 (AAAA-A18-118012390045-2).

References

[1] T. Takenaka, H. Nagata, and Y. Hiruma, Current developments and prospective of lead-free piezoelectric ceramics, *Jpn. J. Appl. Phys.* **47** (5), 3787 (2008). DOI: 10.1143/JJAP.47.3787.

[2] Y. Q. Lu, and Y. X. Li, A review on lead-free piezoelectric ceramics studies in China, *J. Adv. Dielect.* **1** (3), 269 (2011). DOI: 10.1142/S2010135X11000409.

[3] I. Coondoo, N. Panwar, and A. Kholkin, Lead-free piezoelectrics: Current status and perspectives, *J. Adv. Dielect.* **3** (2), 1330002 (2013). DOI: 10.1142/S2010135X13300028.

[4] C. H. Hong *et al.*, Lead-free piezoceramics. Where to move on?, *J. Materiom.* **2** (1), 1 (2016). DOI: 10.1016/j.jmat.2015.12.002.

[5] J. Rodel, and J.-F. Li, Lead-free piezoceramics: Status and perspectives, *MRS Bull.* **43** (8), 576 (2018). DOI: 10.1557/mrs.2018.181.

[6] J.-F. Li *et al.*, (K,Na)NbO_3-based lead-free piezoceramics: Fundamental aspects, processing technologies, and remaining challenges, *J. Am. Ceram. Soc.* **96** (12), 3677 (2013). DOI: 10.1111/jace.12715.

[7] J. G. Wu, D. Q. Xiao, and J. G. Zhu, Potassium-sodium niobate lead-free piezoelectric materials: Past, present, and future of phase boundaries, *Chem. Rev.* **115** (7), 2559 (2015). DOI: 10.1021/cr5006809.

[8] P. K. Panda, and B. Sahoo, PZT to lead-free piezo ceramics, *Ferroelectrics* **474** (1), 128 (2015). DOI: 10.1080/00150193.

[9] Y.-J. Dai, X.-W. Zhang, and K.-P. Chen, Morphotropic phase boundary and electrical properties of $K_{1-}x$Na$x$$NbO_3$ lead-free ceramics, *Appl. Phys. Lett.* **94** (4), 042905 (2009). DOI: 10.1063/1.3076105.

[10] J. Fang *et al.*, Narrow sintering temperature window for (K,Na)NbO_3-based lead-free piezoceramics caused by compositional segregation, *Phys. Stat. Sol. (a)* **208** (4), 791 (2011). DOI: 10.1002/pssa.201026500.

[11] K. Wang, and J.-F. Li, (K,Na)NbO_3-based lead-free piezoceramics: Phase transition, sintering and property enhancement, *J. Adv. Ceram.* **1** (1), 24 (2012). DOI: 10.1007/s40145-012-0003-3.

[12] R. Zuo *et al.*, Sintering and electrical properties of lead-free $Na_{0.5}K_{0.5}NbO_3$ piezoelectric ceramics, *J. Am. Ceram. Soc.* **89** (6), 2010 (2006). DOI: 10.1111/j.1551-2916.2006.00991.x.

[13] S. Zhang, R. Xia, and T. R. Shrout, Modified ($K_{0.5}Na_{0.5}$)NbO_3 based lead-free piezoelectrics with broad temperature usage range, *Appl. Phys. Lett.* **91** (13), 132913 (2007). DOI: 10.1109/ISAF.2008.4693820.

[14] B. Malič *et al.*, Sintering of lead-free piezoelectric sodium potassium niobate ceramics, *Materials (Basel)* **8** (12), 8117 (2015). DOI: 10.3390/ma8125449.

[15] E. D. Politova *et al.*, Influence of NaCl/LiF additives on structure, microstructure and phase transitions of $(K_{0.5}Na_{0.5})NbO_3$ ceramics, *Ferroelectrics* **489** (1), 147 (2015). DOI: 10.1080/00150193.2015.1070248.

[16] E. D. Politova *et al.*, Processing and characterization of lead-free ceramics on the base of sodium-potassium niobate, *J. Adv. Dielect.* **8** (1), 1850004 (2018). DOI: 10.1142/S2010135X18500042.

[17] H. Trivedi *et al.*, Local manifestations of a static magnetoelectric effect in nanostructured $BaTiO_3$-$BaFe_{12}O_9$ composite multiferroics, *Nanoscale* **7** (10), 4489 (2015). DOI: 10.1039/c4nr05657d.